Available online at www.sciencedirect.com
ScienceDirect
Polymer 48 (2007) 2692–2699
polymer
www.elsevier.com/locate/polymer

Positron annihilation lifetime spectroscopy of molecularly imprinted hydroxyethyl methacrylate based polymers

Nikolay Djourelov [a,b], Zeliha Ateş [c], Olgun Güven [c,*], Marijka Misheva [d], Takenori Suzuki [b]

[a] Institute for Nuclear Research and Nuclear Energy, Bulgarian Academy of Sciences, 72 Tzarigradsko shoosse Boulevard, 1784 Sofia, Bulgaria
[b] High Energy Accelerator Research Organization (KEK), 1-1 Oho, Tsukuba, Ibaraki 305-0801, Japan
[c] Department of Chemistry, Hacettepe University, 06532 Beytepe, Ankara, Turkey
[d] Faculty of Physics, Sofia University, 5 J. Bourchier Boulevard, 1126 Sofia, Bulgaria

Received 25 November 2006; received in revised form 9 February 2007; accepted 1 March 2007
Available online 6 March 2007

Abstract

Radiation-induced molecular imprinting of D-glucose onto poly(2-hydroxyethyl methacrylate) (HEMA) matrix was achieved to create three-dimensional cavities to recognize and bind glucose. Molecularly imprinted polymers (MIPs) were synthesized with different types of crosslinkers and varying amounts of template molecule in an attempt to elucidate the impact of imprint quantities on the effectiveness of imprinting technique. The crosslinking agents used in this study were diethylene glycol diacrylate (DEGDA), triethylene glycol dimethacrylate (TEGDMA) and polypropylene glycol dimethacrylate (PPGDMA) in the order of increasing chain length. Crosslinking agent concentration in the polymerization mixture (monomer, crosslinking agent and template) covered a range of 10, 20, 30, and 70 mol%. The mole ratio of template molecule, D-glucose to functional monomer, HEMA, was kept either as 1:3 or 1:6. The absorbed dose varied from 1 to 15 kGy. Control polymers were synthesized with exactly the same composition in the absence of D-glucose. Cavity sizes of MIPs were investigated by positron annihilation lifetime (PAL) measurements. A sandwich arrangement (sample–source–sample) was used. PAL experiments were carried out using a conventional fast–fast coincidence system having a time resolution (FWHM) of about 280 ps. Free-volume hole radii of samples were investigated in their dry and fully water swollen state.

The results obtained from a systematic study of the effects of concentration and molecular size of the crosslinking agents, template to monomer ratio and irradiation dose experiments suggest that control of cavity size is feasible in nanometer scale by the optimization of these parameters revealed by means of (PAL) spectroscopy technique.

Keywords: Positron annihilation lifetime (PAL) spectroscopy; Molecular imprinting; Free volume

1. Introduction

Studies of molecular imprinting involve formation of a pre-polymerization complex between a target molecule and functional monomer or functional polymers with specific chemical moieties capable of specific interactions with target molecule by covalent, non-covalent or both and metal coordination interactions [1–4]. The polymerization reaction is generally initiated in the presence of a crosslinking agent to fix the interstitial geometry imposed by the template (target molecule) which controls size of cavities in the network. After polymerization, the template is removed by solvent-washing procedure and the crosslinked structure retains specific recognition sites and specific moieties for the template molecule.

The free-radical polymerization mechanism is mostly used in these systems for several advantages. The polymerization can be initiated by several factors; thermo or photolytic initiation being the most widely used. Sreenivasan and Sivakumar have also used radiation-induced polymerization technique for imprinting process [5].

Recognition matrices with high substrate selectivity and specificity can be prepared with molecular imprinting

* Corresponding author. Tel.: +90 312 297 7977; fax: +90 312 240 2014.
E-mail address: guven@hacettepe.edu.tr (O. Güven).

0032-3861/$ - see front matter © 2007 Elsevier Ltd. All rights reserved.
doi:10.1016/j.polymer.2007.03.006

technique. A wide range of compounds have been used as imprint molecules to investigate the feasibility of various practical applications. Compounds such as amino acids, proteins, carbohydrates, herbicides and hormones have been used successfully for the preparation of selective recognition matrices [6–10]. Thus, molecularly imprinted polymers have been used as separation and isolation matrices, as antibody and receptor mimics in immunoassay-type analysis, as enzyme mimics in catalytic applications and as biosensor like devices [11–14]. Among these applications, the best developed application area for imprinted materials has been the stationary phases for chromatography.

The success of imprinting process is governed by two factors: chemical affinity of specific chemical structures usually present in the form of pendant groups of monomers toward the template and control of cavity size formed as a result of crosslinked structures. The former provides the chemical and latter, physical recognition hence binding and separation processes.

For chemically similar templates the control of pore size becomes more important for selective separation and binding of molecules of different sizes. The measurement of pore size and its distribution therefore are of great importance in the design of molecularly imprinted polymers.

Yanj and Li used N_2 adsorption method to analyze the pore size and surface area of molecularly imprinted polymers. TEM, AFM and SEM methods were also used to investigate pore size and surface properties of imprinted polymers with physical conformation of either irregular particles or microspheres [15–18]. However, these techniques cannot give precise results about the cavity sizes of MIPs.

Positron annihilation lifetime (PAL) spectroscopy is one of the most sensitive methods of studying free-volume sizes. After entering condensed matter, energetic positron (e^+) becomes thermalized in very short time (some ps), and at the end of its track annihilates on an electron either directly or through forming an intermediate state, positronium. A positronium (Ps) is a bound state of a positron and an electron. Corresponding to the mutual spin orientations (anti-parallel and parallel) of the consisting particles, Ps exists in two states, called *para*-positronium (*p*-Ps) and *ortho*-positronium (*o*-Ps). The intrinsic lifetimes of *p*-Ps and *o*-Ps in vacuum are 0.125 and 142 ns, respectively. In molecular materials, such as polymers, the *o*-Ps is localized in free-volume holes, or cavities, and its positron annihilates on an electron from the surrounding media (the so-called pick-off process). The pick-off annihilation process shortens the *o*-Ps lifetime to some ns. The pick-off annihilation lifetime of the *o*-Ps can be directly correlated to the size of the free-volume holes by a semi-empirical equation proposed by Nakanishi and Jean according to the quantum-mechanical model of Tao later developed by Eldrup et al. [19–21]. The equation correlates the radius, R, of the spherical free-volume hole, where Ps is confined, to the *o*-Ps pick-off annihilation lifetime:

$$\tau_{o\text{-Ps}} = 0.5\left[1 - \frac{R}{R_0} + \frac{1}{2\pi}\sin\left(\frac{2\pi R}{R_0}\right)\right]^{-1}, \quad (1)$$

where $\tau_{o\text{-Ps}}$ is expressed in ns and $\Delta R = R_0 - R = 0.1656$ nm is an empirically determined constant [22]. Although the *o*-Ps lifetime has been successfully correlated to the size of the free-volume hole, its intensity has been found to be influenced by many factors, such as the temperature, positron irradiation, electric field, and polar groups and cannot be used directly as a quantity expressing the concentration of the free-volume holes [23–27].

Our major goal in this work is to determine and control the sizes of free-volume holes produced during the synthesis of glucose imprinted hydroxyethyl methacrylate based polymers by means of PAL spectroscopy. The crosslinking agents of different chain lengths were used in different amounts to induce cavities with different sizes with the anticipation of obtaining the best size for the target molecule, D-glucose. The use of ionizing radiation as the method of generating free radicals for polymerization reactions at room temperature has provided another control over cavity size by simultaneous action of radiation in polymerization and crosslinking reactions.

2. Experimental section

2.1. Materials

The crosslinking agents, diethylene glycol diacrylate (DEGDA) and polypropylene glycol dimethacrylate (PPGDMA with Mn = 560), were purchased from Aldrich (Milwaukee, USA), triethylene glycol dimethacrylate (TEGDMA) was purchased from Aldrich (Steinheim, Germany). The template molecule, D-glucose and functional monomer, 2-hydroxyethyl methacrylate (HEMA) were obtained from Fluka (Buchs, Switzerland). The solvents, dimethyl sulfoxide (DMSO) and ethanol (EtOH), were purchased from Merck (Darmstadt, Germany). All chemicals were of analytical grade and used as received.

2.2. Synthesis of D-glucose imprinted network

All MIP systems with different compositions of template, crosslinking agent and functional monomer were synthesized in the presence of a solvent via radiation polymerization. In order to achieve pre-polymerization complex formation, template molecule, D-glucose, was first mixed with the monomer, then with the crosslinking agent and the solvent. The crosslinking agents used were DEGDA, TEGDMA, PPGDMA in the order of increasing chain length. Crosslinking agent concentration in the polymerization mixture (monomer, crosslinking agent and template) covered a range of 10, 20, 30, and 70 mol%. The mole ratio of D-glucose to functional monomer, HEMA, was kept either as 1:3 or 1:6. Control polymers were synthesized with exactly the same compositions as MIPs in the absence of D-glucose. To investigate the crosslinking effect of radiation, HEMA networks were also prepared without crosslinking agent in the same manner. All MIP systems were prepared in appropriate amount of DMSO:EtOH (3:1 vol:vol) solvent mixture. Once the mixtures mentioned above were prepared they were placed in-between the clamped glass slides

(60 mm × 60 mm × 2 mm) separated with natural rubber ring. Irradiations were carried out in air at ambient temperature in a Gamma cell 220, ^{60}Co-γ irradiator (Nordion, Canada) with an absorbed dose from 1 to 15 kGy. At the end of predetermined irradiation periods the glass slides were placed in deionized water for 6 h, crosslinked polymers then carefully separated from the glass slides and were cut into discs of 12 mm diameter. Discs were then placed into 200 mL of deionized water. The rinsing solutions were changed three times a day to remove the template and unpolymerized material if any. The resulting discs were then dried in air at room temperature and then placed in a vacuum oven ($T = 40$ °C, 100 mbar vacuum), until complete dryness.

2.3. PAL experiments and data analysis

For positron annihilation lifetime (PAL) experiments a positron source was prepared by depositing ca. 1.8 MBq of aqueous ^{22}NaCl on a 7 μm-thick Kapton foil having a 10×10 mm^2 area. After drying, the foil was covered with foil of the same size, and the foil edges were glued with epoxy resin. A sandwich arrangement (sample–source–sample) was used. PAL experiments were carried out using a conventional fast–fast coincidence system having a time resolution (FWHM) of about 280 ps. The measurements were carried out in air at room temperature. The spectra were recorded at every 2 h with total counts in each spectrum being of $\sim 1.8 \times 10^6$. Then, for each type of sample, the first five spectra were summed together resulting in statistics of $\sim 9 \times 10^6$ counts. In a number of experiments on polypropylene and polyethylene, the exposure to the energetic positrons of the weak, radioactive source may lead to increased Ps formation inhibition with the elapsed time of the exposure what is known as source effect [28]. No such sequential change was observed over the timeframe (for some of the samples more than 48 h) of the measurements.

Assuming that e^+ annihilates from states with definite discrete lifetimes, τ_i, the PAL spectrum can be written as:

$$S(t) = R(t) \otimes \left\{ (N_t) \sum_{i=1}^{n} (I_i/\tau_i) \exp(-t/\tau_i) + B \right\}, \qquad (2)$$

where $R(t)$ is the apparatus time resolution function, n is the number of different states, I_i ($\sum_{i=1}^{n} I_i = 1$) denotes the relative intensity of the corresponding component or probability of annihilation with lifetime τ_i, N_t is the total counts, and B is the background. For a continuous distribution of the lifetime, the sum in Eq. (2) has to be replaced by the integral $\int_{\tau=0}^{\infty} (1/\tau) I(\tau) \exp(-t/\tau) \mathrm{d}\tau$, where $\int_{\tau=0}^{\infty} I(\tau) \mathrm{d}\tau = 1$. First, all of the experimental spectra were analyzed by MELT program assuming continuous lifetime distribution [29]. As it was expected, for the short lifetime region (<0.5 ns), two sharp peaks of the lifetime distribution were observed (Fig. 1). The mean lifetime of the first peak was close to 0.125 ns, in good agreement with the p-Ps lifetime. The mean value of the second peak was ~0.380 ns, which is a value usually ascribed to annihilation of free positrons. However, for the longer lifetime region (>0.5 ns), we observed different types of distributions (unimodal or bimodal) even for a single sample (see Fig. 1).

For the case of discrete lifetimes, we used the LT program, and the spectra were resolved first into four components [30]. The experimental errors of the two long lifetimes and their

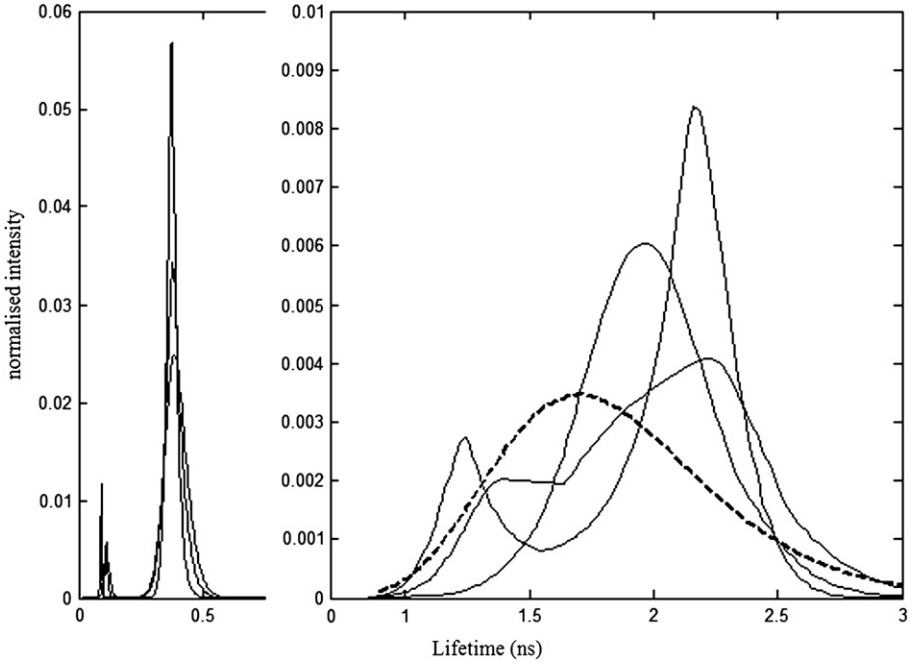

Fig. 1. Example of lifetime distribution for 30% TEGDMA containing sample with 3:1 HEMA:glucose mole ratio and 5 kGy irradiation dose. The continuous lines represent MELT result for consecutive spectra for the same sample with statistics of $\sim 1.8 \times 10^6$ counts. The dashed line is plotted from the third component data obtained by LT from the summed spectrum with statistics of $\sim 9 \times 10^6$ counts.

corresponding intensities were large which lead us to the conclusion that, actually, the two long-lived components represent one component but with a wide distribution. Therefore, for the final analysis, we used the feature of the LT program that allows mixed analysis: two short-lived components were assumed to be discrete and a long-lived component, due to pick-off *o*-Ps annihilation, was assumed to have a log-normal distribution. It should be mentioned that the LT results for the *o*-Ps component differ very little for the consequent spectra of the same sample. That is why the *o*-Ps lifetime distribution only for the summed spectrum is plotted in Fig. 1. For all the samples the standard deviation of the mean lifetime τ_3 with a log-normal distribution obtained by LT program was in the range 0.4–0.5 ns. These data are not presented graphically because there was no clear correlation with the sample preparation conditions.

2.4. Doppler broadening of annihilation gamma-line

For the measurements of the Doppler broadening of the annihilation line, a Ge detector with energy resolution of 1.2 keV at 662 keV line of ^{137}Cs was used. The measurements were performed simultaneously with the PAL measurements. The shape of the Doppler-broadened annihilation γ-line is usually characterized by the integral *S* and *W* parameters. The *S* parameter was defined as the ratio of the sum of counts in the central region of the peak ($|\Delta E| < 0.9$ keV, where ΔE is the shift from the 511 keV peak maximum) relative to the total peak counts (N_{tot}) and the *W* parameter, as the ratio of the sum of counts in the peak wings ($2 < |\Delta E| < 7$ keV) to N_{tot}.

3. Results and discussion

3.1. The effect of type and amount of the crosslinking agent

3.1.1. Dry samples

Fig. 2 shows the mean free-volume hole radius, *R*, and *o*-Ps intensity versus the type of crosslinking agent at different concentrations. The presented results are for dry samples with fixed HEMA/glucose (H:G = 3:1) ratio and gamma-irradiation dose ($D = 5$ kGy). The values for the radii are calculated by iteration procedure based on Eq. (1).

The results shown in Fig. 2 can be evaluated under two categories: low ($C = 10$ and 20%) and high ($C = 30$ and 70%) concentration of the crosslinking agent. When the concentration is low, *R* is slightly affected by the molecular size of the crosslinking agent, as we go from pure HEMA (denoted by NA on the figures) crosslinked by gamma rays only to HEMA crosslinked in the presence of DEGDA, there is an increase of about 0.01 nm in the radius of holes. We can explain this behavior with the purely random crosslinking of HEMA alone resulting in dense crosslinking whereas in the presence of DEGDA the two functionality of the crosslinking agent imposes a certain limited mesh size on the crosslinked structure. In the same concentration range by increasing the size of the crosslinking agent from DEGDA to TEGDMA, *R* does not seem to be affected much if not slightly decreasing. Although by going from DEGDA to TEGDMA there is an increase of one ethylene glycol unit on the chain, this small increase in size is compensated by the presence of methyl group of methacrylate. The increase in *R* in the presence of PPGDMA as compared to other crosslinking agents is clear from the figure, which is simply related to rather big difference in their respective chain lengths. But still the effect of PPGDMA is not as big as expected which can be related to dominating structure of randomly crosslinked HEMA in this range, comprising 80 and 90% by mole of the total.

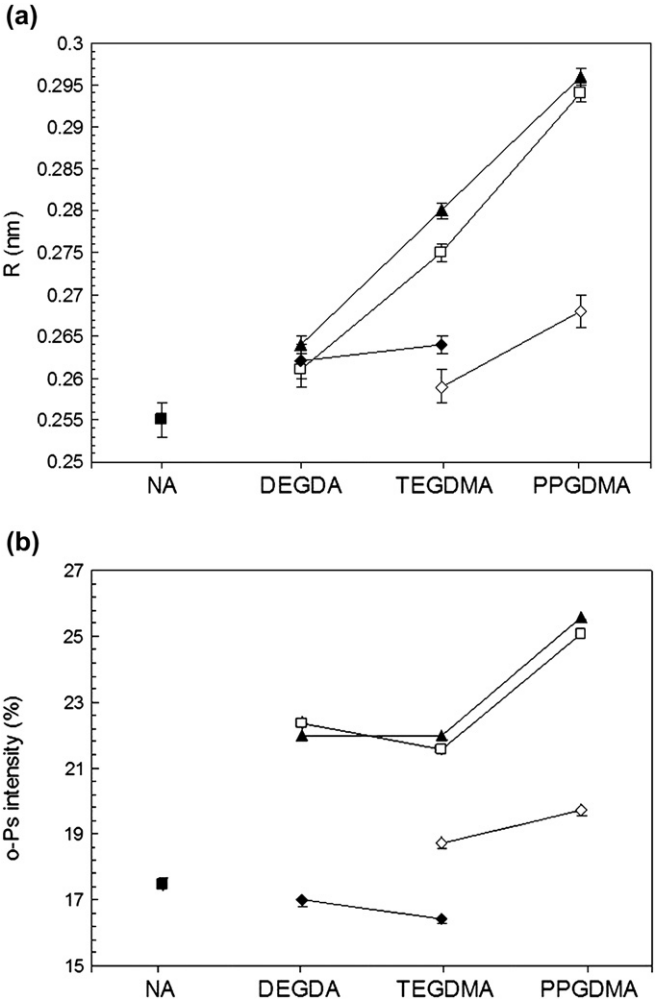

Fig. 2. Free-volume hole radius (a) and *o*-Ps intensity (b) for dry samples versus the type of crosslinking agent at different concentrations. Irradiated samples ($D = 5$ kGy) with 3:1 HEMA:glucose mole ratio; symbols ▲, □, ◇, ◆, and ■ indicate 70, 30, 20, 10% and no crosslinking agent containing samples, respectively. NA indicates sample prepared without crosslinking agent.

In the high concentration range of crosslinking agents ($C = 30$ and 70%), however, the change of *R* with crosslinking agent type is obvious as seen from Fig. 2a. *R* steadily increases by going from DEGDA to TEGDMA and to PPGDMA from about 0.26 to 0.28 and to 0.30 nm, respectively. In this crosslinking agent concentration range, HEMA is in rather low amounts as compared to the crosslinking agent and the overall structure of crosslinked system is dominated by the

polymerization of crosslinking agent itself resulting in mesh sizes imposed by the lengths of crosslinking agents. A comparison of the relative sizes of free volumes in the swollen state of MIPs can be made by measuring the equilibrium swelling degrees of these crosslinked systems. In parallel with PAL spectroscopic studies, the swelling behaviors of MIPs were also investigated. Fig. 3 shows the swelling kinetics of three MIPs in water. The equilibrium swelling ratios obtained for HEMA crosslinked in the presence of 30% of DEGDA, TEGDMA and PPGDMA were 37, 43 and 82%, respectively, as shown in Fig. 3, which show a good correlation with free-volume hole radii of dry samples as given above.

3.1.2. Samples swollen in water

Fig. 4 shows the PAL spectroscopic results for the same MIP samples used in Fig. 2, this time fully swollen in water. R versus crosslinking agent type graph given in Fig. 4a reveals an interesting result. Irrespective of the chain length of crosslinking agent and its concentration, the free-volume hole radius determined for these MIPs was found to be the same for all systems. Water absorption and consequent changes in free-volume characteristics in polymers are widely studied by PAL spectroscopy [31–35]. With an increase of water content in the polymer an increase in the sizes of free-volume holes has been observed. This has been explained by the plastification effect (enhanced polymer chain mobility) of the water molecules absorbed at the inner surfaces of free-volume holes. What is measured by PAL spectroscopy in these studies is the free volume not occupied by water. At higher water concentration, the o-Ps lifetime reaches a saturation value that corresponds to free-volume hole radius of 0.28 nm. The last value is the Ps-bubble size in water at room temperature which means that Ps is formed in bulk water fully or partially occupying the free-volume holes in the water swollen samples [36].

The decrease of free-volume hole size after swelling for the samples prepared with PPGDMA, $C = 30$ and 70% (Fig. 4a) indicates that the free-volume holes inside the swollen crosslinked polymeric system are larger than the Ps-bubble size and probably fully occupied with water. For the rest of the samples, an increase can be seen in the free-volume size as compared to dry samples because of the swelling. Therefore for the last-mentioned samples plastification effect is the other possible explanation for the observed hole size enhancement. However, because of the almost constant R-values for the swollen samples, we are inclined to believe that what is measured for all of the swollen samples is the size of the Ps-bubble in water which occupies the free-volume holes. This conclusion has also lead us to propose that the pores created during formation of MIPs are not closed but all interconnected giving access to diffusion of water. The presence of interconnected pores instead of or together with discrete ones may be expected to cause a slight increase in the estimated pore sizes. As Ps is formed in such systems, it may diffuse through the interconnected pores to find the largest one which is

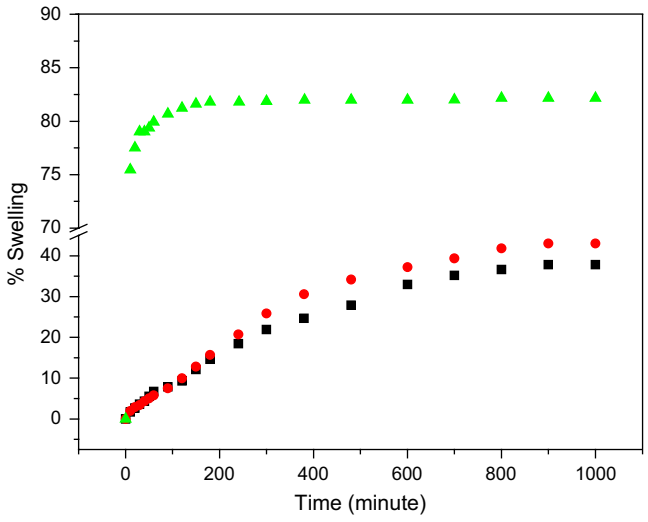

Fig. 3. Swelling experiments in water for imprinted polymers crosslinked with 30% of DEGDA (■), TEGDMA (●), PPGDMA (▲).

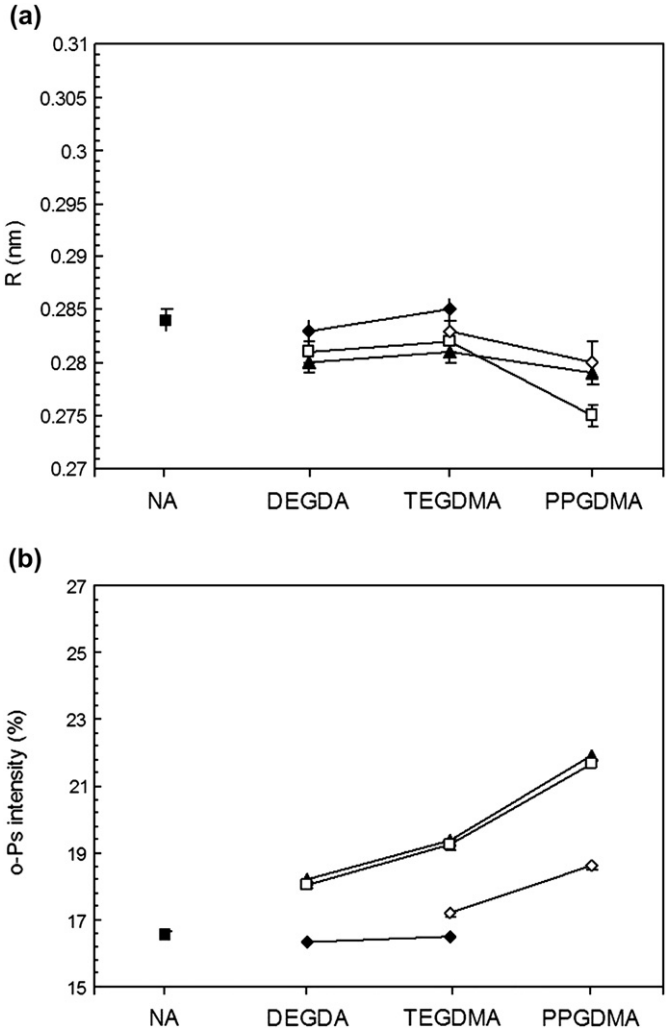

Fig. 4. Free-volume hole radius (a) and o-Ps intensity (b) for water swollen samples versus the type of crosslinking agent at different concentrations. Irradiated samples ($D = 5$ kGy) with 3:1 HEMA:glucose mole ratio; symbols ▲, □, ◇, ◆, and ■ indicate 70, 30, 20, 10% and no crosslinking agent containing samples, respectively. NA indicates sample prepared without crosslinking agent.

energetically the most favorable for Ps thus giving rise to slightly overestimated mean sizes for the pores.

O-Ps intensity (Figs. 2b and 4b) is a quantity directly connected to the Ps formation probability. Although Ps formation probability depends mostly on the available free-volume holes, it is affected by many additional factors as discussed in Section 1. For the studied samples, the main factor is the presence of polar groups in the chemical structure of the sample precursors. The electro-negativity of oxygen atom is 3.5 P.u., while that for hydrogen and carbon is 2.1 and 2.5, respectively. Therefore, groups like C═O and COH express definite polarity, and oxygen is partially negatively charged. Thus, positrons are attracted by the oxygen of these groups and Ps formation is inhibited. If the difference can be neglected for the polarity of the different oxygen containing groups, an estimation can be made roughly for the oxygen effect on the *o*-Ps intensity by calculating the fraction of the oxygen weight over the total molecular weight of HEMA and the crosslinking agents. This fraction is 0.20, 0.31, 0.35, and 0.08 for HEMA, DEGDA, TEGDMA, and PPGDMA, respectively. That is why both effects on the actual change in the number of free-volume holes and Ps inhibition have to be considered carefully. If we consider only the oxygen effect because of the presence of DEGDA and TEGDMA crosslinking agents on the *o*-Ps intensity we should observe a decrease from the values for HEMA samples. However, the observed change is an increase (Figs. 2b and 4b). So, it could be concluded that there is increase in the free-volume holes' number due to crosslinking which is evident for higher crosslinking agent concentrations ($C = 30$ and 70%), while for the lower concentrations ($C = 10$ and 20%) it is not clear. The *o*-Ps intensity value for the PPGDMA crosslinking agent is higher compared with those for the other crosslinking agents but this does not surely mean higher number of free-volume holes. Most probably this comes from the lower oxygen content in PPGDMA.

Additional confirmation of the last suggestion comes from the plot of *S* parameter as a function of *W* parameter (see Fig. 5) obtained from DBAL experiments. *S* parameter depends mostly on the Ps yield, while *W* parameter is sensitive to the chemical structure of the sample. For our choice of the energy range for *W* parameter calculation, *W* parameter is highly sensitive to annihilation on oxygen [36,37]. Although the experimental data scattering in Fig. 5 is high, it can be seen that the trend lines of the sample groups prepared with PPGDMA (dry and swollen) differ from the rest of the sample groups. The slopes of the trend lines for these two groups are approximately −1.70, while those for the other groups lie in the range −1.33 to −1.17. This means that for the same decrease of the Ps yield (*S* parameter decrease) the increase in *W* parameter for PPGDMA containing samples is lower than that for the other group of samples. The reason is that fewer positrons are trapped and annihilate on oxygen in the samples prepared with PPGDMA than that in the samples prepared with TEGDMA and DEGDA, and in pure HEMA, because of the relatively less oxygen content of propylene groups.

3.2. The effect of template concentration

Fig. 6 shows the effect of template concentration on the free-volume hole radius and number of MIPs. Two classes of samples are considered, those prepared from pure HEMA only by radiation-induced crosslinking denoted by NA (see the caption of the figures, solid and empty circles) and those prepared from HEMA − TEGDMA ($C = 30\%$) and glucose where the HEMA to glucose concentrations were kept at 3:1 and 6:1. PAL spectra of all these samples were taken in both dry and swollen states. In dry state, although small but still a difference was observed for imprinted (those with the template, H:G = 6:1 and 3:1) and non-imprinted (H:G = 6:0 and 3:0) samples. The free-volume hole radius of imprinted

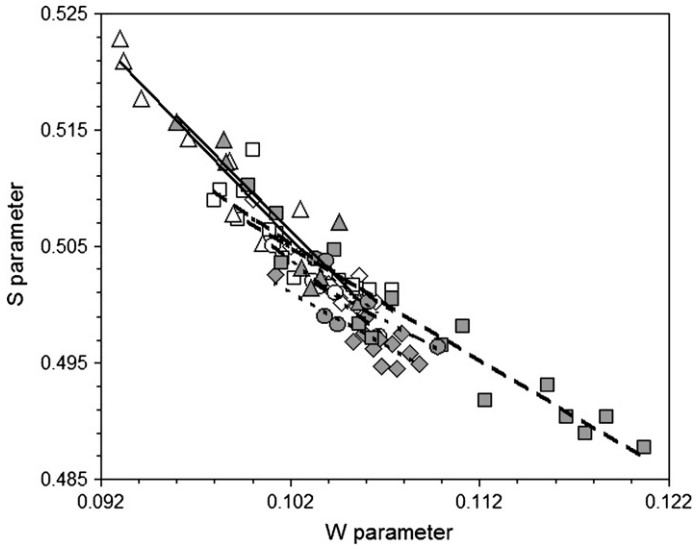

Fig. 5. *S* parameter as a function of *W* parameter. Horizontal and vertical error bars (not drawn for clearness) for *S* and *W* are about twice the size of the points. The lines are linear fits of the corresponding groups of experimental points; (◇) NA, (◆) NA swollen, (□) TEGDMA, (■) TEGDMA swollen, (△) PPGDMA, (▲) PPGDMA swollen, (○) DEGDA, (●) DEGDA swollen, (----) linear NA and linear NA swollen, (−−) linear TEGDMA and linear TEGDMA swollen, (——) linear PPGDMA and linear PPGDMA swollen, (—·---) linear DEGDA and linear DEGDA swollen.

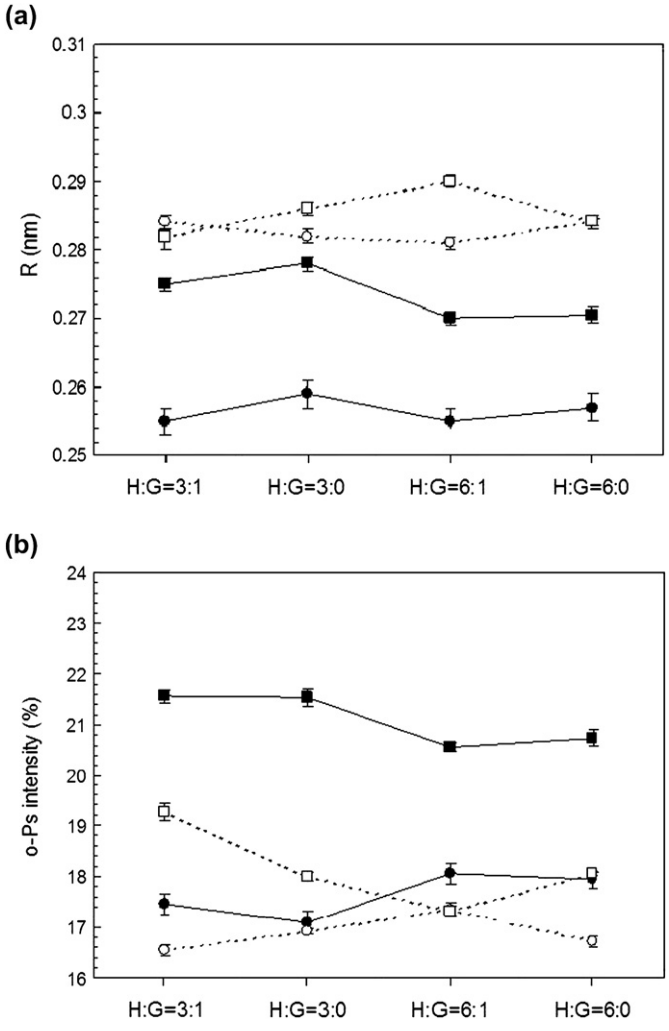

Fig. 6. Free-volume hole radius, R (a) and o-Ps intensity (b) versus HEMA/glucose (H:G) ratio. NA indicates samples prepared without crosslinking agent. Irradiated samples ($D = 5$ kGy) with 3:1 and 6:1 HEMA:glucose mole ratio; symbols ●, ○, ■, and □ indicate NA in dry state, NA in swollen state, 30% TEGDMA in dry state, and 30% TEGDMA in swollen state, respectively.

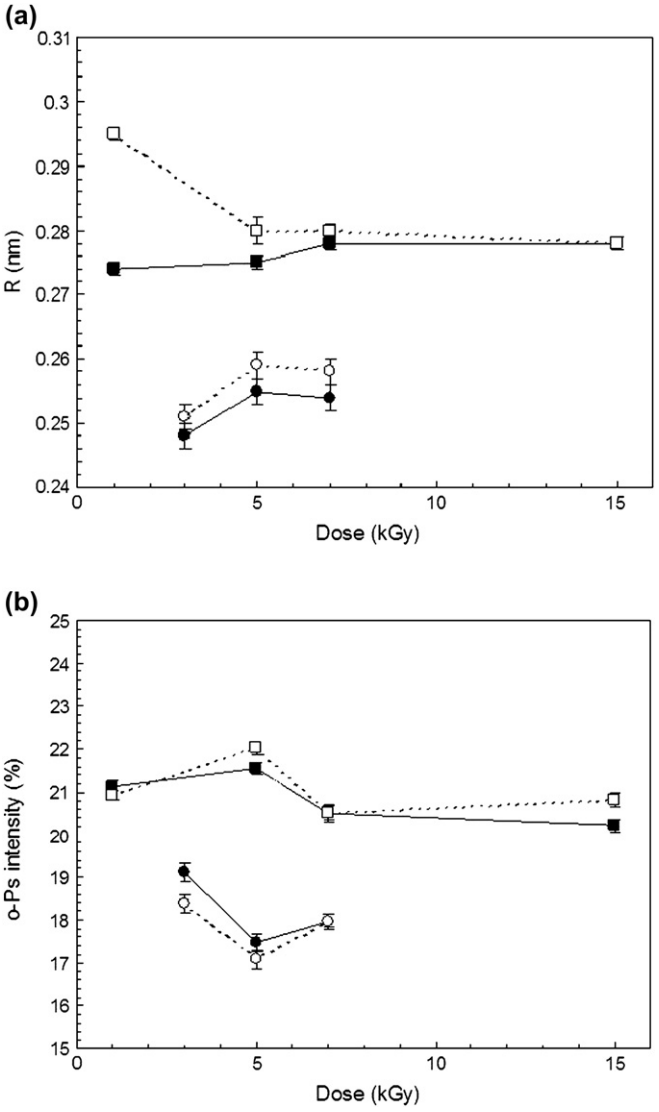

Fig. 7. Free-volume hole radius, R (a) and o-Ps intensity (b) versus irradiation dose. NA indicates samples prepared without crosslinking agent. Samples with 3:1 HEMA:glucose mole ratio; symbols ●, ○, ■, and □ indicate glucose imprinted NA, non-imprinted NA, glucose imprinted 30% TEGDMA containing sample, and non-imprinted 30% TEGDMA containing sample with varying dose, respectively.

samples was found to be smaller than non-imprinted ones which shows that the presence of template brings a control of cavity volume though small in magnitude. In swollen samples since what is measured is the dimension of the Ps-bubble in water filling the free-volume holes, the R-value does not change much with neither crosslinking agent nor template ratio. In fact the equilibrium swelling ratios of non-imprinted HEMA only samples with different template ratios were almost the same, 69 and 71% indicating that even in the expanded state they do not differ much in volume.

3.3. The effect of radiation dose

The change of R with dose as shown in Fig. 7 is given only for samples prepared in the presence of TEGDMA and shows that for non-imprinted samples R is smallest at the lowest dose and become independent of dose beyond 5 kGy. This is an expected result since the lower the dose, the less will be the concentration of crosslinks, thus wider will be the space between the chains. With increasing dose crosslink density will increase and beyond a certain dose considering the chain scission effect of radiation as well it will reach a saturated value.

4. Conclusions

Positron annihilation lifetime (PAL) experiments presented in this study are the first attempt at molecular imprinting to analyze cavity size in nanometer scale. The free-volume hole measurement for D-glucose imprinting in a polymer matrix via PAL spectroscopy demonstrated in this study shows the power of this technique in analyzing the success of molecular imprinting process.

In this study, D-glucose imprinted networks were synthesized with different crosslinkers by using radiation-induced polymerization. For the optimization of free-volume holes in imprinted network, crosslinkers with different chain lengths selected and varying amounts were used with two different template-functional monomer ratios. The use of ionizing radiation as the tool for initiation of polymerization and copolymerization provided an additional parameter for controlling of network structure. These results demonstrate the feasibility of measuring and thus controlling cavity size in an imprinting system based on various parameters.

Acknowledgements

The first author (N.D.) was supported by Japan Society for the Promotion of Science fellowship. M.M. and O.G. appreciate support of the IAEA through CRP 'Controlling of degradation effects in radiation processing of polymers' for the establishment of a collaboration between respective laboratories. O.G. appreciates the support of the Academy of Sciences of Turkey.

References

[1] Wizeman WJ, Kofinas P. Biomaterials 2001;22:1485–91.
[2] Wulff G. Angewandte Chemie International Edition in English 1995;34:1812–32.
[3] Sellergren B. Trends in Analytical Chemistry 1997;16:6.
[4] Sellergen B, Andersson LI. Methods 2000;22:92–106.
[5] Sreenivasan K, Sivakumar R. Journal of Applied Polymer Science 1999;71:1823–6.
[6] Andersson L, Sellergren B, Mosbach K. Tetrahedron Letters 1984;25:5211–4.
[7] Bodugöz H, Güven O, Peppas NA. Journal of Applied Polymer Science 2007;103:432–41.
[8] Wulff G, Schauhoff S. Journal of Organic Chemistry 1991;56:395–400.
[9] Byrne ME, Oral E, Hilt ZJ, Peppas N. Polymers for Advanced Technologies 2002;13:798–816.
[10] Panasyuk-Delaney T, Mirsky VM, Ulbrich M, Wolfbeis OS. Analytica Chimica Acta 2001;435:157–62.
[11] Zi-Hui M, Qin L. Analytica Chimica Acta 2001;435:121–7.
[12] Ye L, Mosbach K. Reactive and Functional Polymers 2001;48:149–57.
[13] Chianella I, Piletsky SA, Tothill IE, Chen B, Turner APF. Biosensors and Bioelectronics 2003;18:119–27.
[14] Haupt K, Mosbach K. Chemical Reviews 2000;100:2495–504.
[15] Yoshimi Y, Ohdaira R, Iiyama C, Sakai K. Sensors and Actuators, B 2001;73:49–53.
[16] Ye L, Cormack PAG, Mosbach K. Analytica Chimica Acta 2001;435:187–96.
[17] Piscopo L, Prandi C, Coppa M, Sparnacci K, Laus M, Laganå A, et al. Macromolecular Chemistry and Physics 2002;203:1532–8.
[18] Sellergren B, Wieschemeyer J, Boos K, Seidel D. Chemistry and Materials 1998;10:4037–46.
[19] Nakanishi H, Jean YC. Positrons and positronium in liquids. In: Schrader DM, Jean YC, editors. Positron and positronium chemistry. Amsterdam: Elsevier Science; 1988. p. 159.
[20] Tao SJ. Journal of Chemical Physics 1972;56:5499.
[21] Eldrup M, Pedersen NJ, Sherwood JN. Physical Review Letters 1979;43:1407.
[22] Nakanishi H, Wang SJ, Jean JC. In: Sharma SC, editor. Positron annihilation studies of fluid. Singapore: World Scientific; 1988. p. 292.
[23] Peng ZL, Olson BG, Mc Gervery JD. Polymer 1999;40:3033.
[24] Suzuki T, Ito Y, Kondo K. Radiation Physics and Chemistry 2001;60:535.
[25] Kobayashi Y, Wang CL, Hirata K. Physical Review B 1998;58:5384.
[26] Suzuki T, He C, Shantarovich V, Kondo K, Hamada E, Matsuo M, et al. Radiation Physics and Chemistry 2003;66:161.
[27] Maurer FHJ, Schmidt M. Radiation Physics and Chemistry 2000;58:509–12.
[28] Peng ZL, Itoh Y, Li SQ, Wang SJ. Physical Status Solidi A 1996;155:299.
[29] Shukla A, Hoffmann L, Manuel AA, Peter M. Materials Science Forum 1997;255:233.
[30] Kansy J. Nuclear Instruments and Methods in Physics Research Section A 1996;374:235.
[31] Hodge RM, Simon GP, Whittaker MR, Hill DJT, Whittaker AK. Journal of Polymer Science, Part B Polymer Physics 1998;36:463–71.
[32] Ito K, Ujihira Y, Higa M. Materials Science Forum 1997;255–257:305–7.
[33] Dlubek G, Buchhold R, Hubner Ch, Nakladal A. Macromolecules 1999;32:2348–55.
[34] Suzuki T, Oki Y, Numajiri M, Miura T, Kondo K, Dshiomi Y, et al. Polymer 1996;37:3025–30.
[35] Ito Y, Sanchez V, Lopez R, Fucugauchi L, Tanaka K, Okamoto K. Bulletin of the Chemical Society of Japan 1993;66:727–32.
[36] Kenji I, Yusuke U, Takashi Y, Kazuyuki H. Polymer 1999;40:4315–23.
[37] Nagai Y, Nonaka T, Hasegawa M, Kobayashi Y, Wang CL, Zheng A, et al. Physical Review B 1999;60:11863–6.